MOLECULAR AND CELLULAR BIOLOGY, June 2009, p. 2997–3006 Vol. 29, No. 11
0270-7306/09/$08.00+0 doi:10.1128/MCB.01008-08

Integrating Receptor Signal Inputs That Influence Small Rho GTPase Activation Dynamics at the Immunological Synapse▽†

Konstantina Makrogianneli,[1,2]‡ Leo M. Carlin,[1,2]‡ Melanie D. Keppler,[1,2] Daniel R. Matthews,[1,2] Enyinnaya Ofo,[1,2] Anthony Coolen,[3] Simon M. Ameer-Beg,[1,2] Paul R. Barber,[4] Borivoj Vojnovic,[4] and Tony Ng[1,2]*

Richard Dimbleby Department of Cancer Research[1] and Division of Cancer Studies and Randall Division of Cell & Molecular Biophysics,[2] King's College London, Guy's Medical School Campus, London SE1 1UL, United Kingdom; Department of Mathematics, King's College London, Strand Campus, London WC2R 2LS, United Kingdom[3]; and University of Oxford, Gray Cancer Institute, Mount Vernon Hospital, Northwood HA6 2JR, United Kingdom[4]

Received 26 June 2008/Returned for modification 6 November 2008/Accepted 9 March 2009

The Rho GTPase Cdc42 regulates cytoskeletal changes at the immunological synapse (IS) that are critical to T-cell activation. By imaging fluorescent activity biosensors (Raichu) using fluorescence lifetime imaging microscopy, Cdc42 activation was shown to display kinetics that are conditional on the specific receptor input (through two IS-associated receptors, CD3 and β1 integrin). CD3-triggered Cdc42 activity is dependent on the cyto-2 (NPIY) motif of the β1 integrin cytoplasmic domain. Perturbations of the ezrin-radixin-moesin (ERM) function blocked CD3- and β1-dependent increases in Cdc42 activity. Both IS-associated receptors probably lie on a serial molecular pathway and transduce signals through the ERM-dependent machinery that is responsible for the remodeling and stabilization of the synapse. Cdc42 activity is impaired in β1 integrin-deficient T cells that form conjugates with antigen-presenting cells but is partially restored in the context of an antigen-specific synapse. This restoration of Cdc42 activity is due, at least in part, to the recruitment and activation of β2 integrin.

Our understanding of immune surveillance has been advanced by the discovery and characterization of the immunological synapse (IS) formed between T lymphocytes and antigen-presenting cells (APC). The formation of the immune synapse is known to involve the segregation of molecules, leading to (i) the formation of a central T-cell receptor (TcR)-peptide-loaded major histocompatibility complex (pMHC) cluster, known as the central supramolecular activation cluster (cSMAC); (ii) a peripheral adhesion ring junction (pSMAC) made up of adhesion molecules that include integrins (specifically LFA-1 [αLβ2] and VLA4 [α4β1]) and adaptor proteins such as talin; and (iii) a distal zone rich in CD45 (16).

Integrins are a family of heterodimeric transmembrane receptors that mediate cell-cell interaction, cell adhesion to extracellular matrix, and cell migration (reviewed in reference 25). In migrating T lymphocytes, β1 integrins such as VLA4 were shown to cluster at the uropod/distal pole complex (DPC) (38). DPCs are cytoskeletal structures in the retractile pole opposite the site of cell-cell contact in activated T cells. This is in contrast to LFA-1 integrins, which were clustered mainly in the leading pseudopodia of these migrating cells (62).

During IS formation, critical interactions are made with the cytoskeleton. Evidence suggests that actin assembly at the cell-cell interaction site is nucleated by the Arp2/3 complex and/or formins, following activation by Rho GTPases such as Cdc42 and Rac1 (16, 28). In the context of the pSMAC, Rac1 and branched actin polymers have been identified in various models as being responsible for the formation of forward-probing membrane structures (15). In T cells triggered by APC presenting low levels of antigenic peptides, Cdc42 and/or its downstream effector Wiskott-Aldrich syndrome protein (WASP) are involved in the recruitment of protein kinase Cθ (PKCθ) and talin to the cSMAC and pSMAC, respectively (10). In a recently published functional atlas of the integrin adhesome (65), integrins are physically linked to actin through adaptors and binding proteins and are functionally associated with regulators of Rho GTPases (GTPase-activating proteins [GAPs] and guanine nucleotide exchange factors [GEFs]). They thereby can provide an intriguing intersection between cytoskeletal remodeling and adhesion controls at the IS. Understanding the molecular organization of the T-cell-APC interaction requires a detailed knowledge of the spatiotemporal relationship between the cytoskeleton, adhesion molecules, antigen receptors, and costimulatory receptors during different stages of the cell-cell contact.

Members of the ezrin-radixin-moesin (ERM) family of proteins play an important regulatory role during IS formation (18, 58) and T-cell activation by aiding the formation of the DPC, a structure that is essential for T-cell activation (reviewed in reference 15). In the context of lymphocyte signaling via the integrins, the cross-linking of ICAM-2 by LFA-1 has been shown to induce ezrin phosphorylation and enhance ezrin-ICAM interaction (49). Ezrin also has been shown to cocluster with the TcR and PKCθ in anti-CD3-stimulated

* Corresponding author. Mailing address: King's College London, 2nd Floor, New Hunt's House, Guy's Medical School Campus, London SE1 1UL, United Kingdom. Phone: 44 (0) 20 7848 8056. Fax: 44 (0) 20 7848 6435. E-mail: tony.ng@kcl.ac.uk.

† Supplemental material for this article may be found at http://mcb.asm.org/.

‡ These authors contributed equally to this work.

▽ Published ahead of print on 23 March 2009.

Jurkat T cells (26). In the same work, ezrin was shown to directly interact with and recruit ZAP-70 to the IS.

MATERIALS AND METHODS

Cell lines. Human Jurkat T and lymphoblastoid Raji B cell lines were obtained from the ATCC. The β1 integrin-negative Jurkat A1 line was a kind gift from Y. Shimizu (University of Minnesota Medical School). The levels of expression of other receptors (such as the β2 integrin LFA-1, TcR/CD3, CD2, and CD28) by this A1 mutant cell line were similar to those of wild-type (WT) Jurkat cells. The A1-derived lines reconstituted with the WT and mutant β1 integrin constructs (A1β1-WT, A1β1-ΔNPKY, A1β1-ΔNPIY, and A1β1-793 [with the last five amino acids deleted]) (57) were gifts from M. Alessandra Rosenthal-Allieri, A. Bernard (Université de Nice Sophia-Antipolis), and Y. Shimizu (with permission from M. Ginsberg). The WT Jurkat and A1 lines were cultured in RPMI 1640 medium (Sigma) and then supplemented with 10% heat-inactivated fetal bovine serum (Biosera), 1% glutamine (PAA), 100 U/ml penicillin (PAA), and 100 μg/ml streptomycin (PAA) at 37°C in a humidified 5% CO_2 atmosphere. In addition, A1β1-WT, A1β1-ΔNPKY, A1β1-ΔNPIY, and A1β1-793 lines were maintained in medium containing 1 mg/ml G418 (PAA) to maintain the stable expression of β1 integrin constructs.

Plasmids and cell transfection. The ezrin constructs (described previously [23, 53]) were subcloned in the pCB6 vector containing the vesicular stomatitis virus G (VSV-G) tag (the vector is described in reference 1). For transfection, the cells were subcultured the day before electroporation in a 1:2 ratio. Cells (10^7) were electroporated in 250 μl serum-free RPMI medium containing 40 μg of plasmid DNA and 25 mM HEPES (PAA) at 260 V and 960 μF using the Gene Pulser II electroporation system (Bio-Rad). All cell lines were allowed to express constructs for 24 h.

Construction and utility of red fluorescent protein (RFP)-Raichu-GFP biosensors. Yellow fluorescent protein-Raichu-cyan fluorescent protein (YFP-Raichu-CFP) probes for reporting localized small Rho GTPase activities (Cdc42, Rac1, and RhoA) in cells have been reported previously (27) and were obtained from M. Matsuda (Osaka University, Japan). The original Raichu probes were designed for the intensity measurements of sensitized acceptor emission to detect fluorescent resonance energy transfer (FRET) (20). The benefits of using donor fluorescence lifetime imaging microscopy (FLIM) to detect FRET are that it is independent of fluorophore concentration, donor-acceptor stoichiometry, and light path length and therefore is well suited to studies in intact cells (43, 44, 63, 64). In the absence of FRET, CFP emission exhibits a biexponential decay and is unsuitable for quantitative fluorescence lifetime-based FRET assays (40). Therefore, CFP and YFP in the original Raichu probes were replaced with green fluorescent protein (GFP) and mRFP1 as the donor and acceptor fluorophores, respectively.

The RFP-Raichu-GFP sensor was synthesized by the excision of the sensor module between YFP and CFP and insertion between the mRFP1 and enhanced GFP (EGFP) (in the pEGFP-N1 vector [Clontech] that has been modified by the addition of mRFP1 and altering the multiple cloning site). The membrane-targeting CAAX sequence was cloned after the EGFP, with the resulting construct maintaining the same linkers as the original. The resultant GFP- and mRFP1-tagged Raichu constructs retain the original design of the CFP/YFP-tagged version, i.e., mRFP1-PBD-GTPase-GFP-CAAX (http://www.path1.med.kyoto-u.ac.jp/mm/e-phogemon/vector.htm and reference 41).

Upon GTP binding, Rac1 and Cdc42 exhibit a higher affinity toward the Cdc42- and Rac-interactive binding (CRIB) domain of PAK1, bringing the two different fluorescent proteins of the biosensor into close proximity and enabling FRET between GFP and mRFP1. FRET results in a decrease in the observed GFP fluorescence lifetime (τ). Since Raichu-Rac1 and Raichu-Cdc42 cannot bind to Rho-guanine dissociation inhibitor (two [underlined] of the four residues $H^{103}H^{104}\underline{K}^{184}\underline{R}^{186}$ in Cdc42 and HH<u>KK</u> in Rac1 that are required for Rho-guanine dissociation inhibitor binding are truncated [24]), these probes provide only the quantitation of the balance between GEFs and GAPs at the membrane.

Antibody stimulation and IS formation assay. Anti-CD3 (UCHT1), stimulatory anti-CD11a (TS2/4.11), and blocking anti-CD11a (MAb 38) monoclonal antibodies (MAb) were obtained from the Cancer Research UK Monoclonal Antibody Service. The use of the activating anti-β1 integrin (12G10; a kind gift from Martin Humphries, University of Manchester) and/or anti-CD3 antibodies immobilized onto surfaces by anti-mouse immunoglobulin G (IgG) Fc $F(ab')_2$ fragments to stimulate T cells has been described previously (45, 46). Jurkat-Raji conjugates were prepared according to an established protocol (60), with some adaptations. Briefly, Raji B cells at a density of 5×10^6/ml were preloaded with *Staphylococcus* enterotoxin E (SEE; Toxin Technology). Jurkat cells (2×10^5) were incubated with equal numbers of Raji at 37°C for the required time periods. The combined cell suspension then was centrifuged at 1,000 rpm for 5 min and then resuspended gently with Cytofix/Cytoperm (a fixative and permeabilization agent; BD Pharmingen) for 5 min at 4°C and washed twice with phosphate-buffered saline (PBS). For the LFA-1 blocking experiments, Raichu-Cdc42-transfected A1 and A1β1-WT T cells were preincubated in the presence or absence of 10 μg/ml anti-LFA-1 blocking MAb (MAb 38) for 45 min at 37°C, 5% CO_2 and then allowed to form conjugates with SEE-loaded or unloaded Raji APC as described above (the blocking anti-LFA-1 MAb was present at 10 μg/ml throughout). Fixed cells were allowed to attach to poly(L)-lysine-coated chamber slides (Nunc) overnight at 4°C before mounting.

FRET determination by multiphoton FLIM. Time-domain FLIM was performed with a multiphoton microscope system comprising a solid-state pumped (8-W Verdi; Coherent), femtosecond self-modelocked Ti:Sapphire (Mira; Coherent) laser system, an in-house-developed scan head, and an inverted microscope (Nikon TE2000E) as described previously (50). In the first instance, the presence/absence of FRET is monitored by the following equation: conventional FRET efficiency (FRET Eff) = $1 - \tau_{da}/\tau_{control}$, where τ_{da} is the lifetime of GFP-Raichu-RFP and $\tau_{control}$ is GFP-Cdc42/Rac1 lifetime measured in the absence of acceptor. Pixel-by-pixel lifetime determination was achieved using a modified Levenberg-Marquardt fitting technique (7). For cases where sufficient reduction in the measured lifetime indicated FRET, an additional analysis was performed. Applying a biexponential fluorescence decay model and global analysis techniques to the data enables the determination of fluorescence lifetimes for spatially invariant noninteracting ($\tau_{control}$) and interacting (τ_{FRET}) subpopulations and their preexponential factors (or relative concentration) on a pixel-by-pixel basis (8). The FRET population F_2 (see Fig. S2B in the supplemental material) is the fraction of interacting molecules that exhibit τ_{FRET} according to the equation τ_{FRET} = FRET Eff/$[1 - (\tau_{FRET}/\tau_{control})]$, since $\tau_{da} = F_2 \times \tau_{FRET} + (1 - F_2) \times \tau_{control}$.

RESULTS

Cdc42 is differentially activated via CD3 or β1 integrin, whereas Rac1 activity shows no significant difference between stimuli. To investigate the spatiotemporal dynamics of Rho GTPase activation in T cells activated by receptor-specific signals, we have reengineered original fluorescent activity biosensors (Raichu probes) (27) to monitor the levels of Cdc42 and Rac1 activities by FLIM/FRET techniques (see Materials and Methods and references 2, 5, 12, 21, 32, 42–44, 47, 48, 50, and 53). The Raichu biosensors for Cdc42 and Rac1 are known to exhibit a baseline FRET as a result of the finite separation between the two fluorescent proteins when the biosensor is in the open conformation (27). For unstimulated controls, we measured the GFP fluorescence lifetime of Raichu-Rac1- or Raichu-Cdc42-expressing Jurkat T cells adhered to anti-CD43 coated coverslips before fixation or fixed with paraformaldehyde in suspension and cytospun onto a slide before mounting (Fig. 1A, D). By using FLIM to monitor the FRET changes, we observed a statistically significant increase in Cdc42 activity in response to anti-β1 integrin after 10, 30, and 120 min of adherence compared to that of anti-CD3 antibody activation (Fig. 1B to D). Cumulative analyses of four experiments (n = 15 cells) are shown in Fig. 1D. No significant difference in Rac1 activity between anti-β1 integrin- and anti-CD3-stimulated cells was observed at these time points (Fig. 1D). A dynamic mathematical model simulating the kinetics of Rho GTPase activation was used to analyze these experimental datasets (see Fig. S2 in the supplemental material).

As an additional control to establish the utility of the GFP-Raichu-RFP Cdc42 probe, a Raichu probe containing a Thr^{17}-to-Asn (T17N) mutation, known to have a much-reduced affinity for GTP (19), was expressed in Jurkat cells. WT Raichu-Cdc42 has an ~2.4-fold increase in mean FRET efficiency compared to that of T17N Raichu-Cdc42 after 30 min of

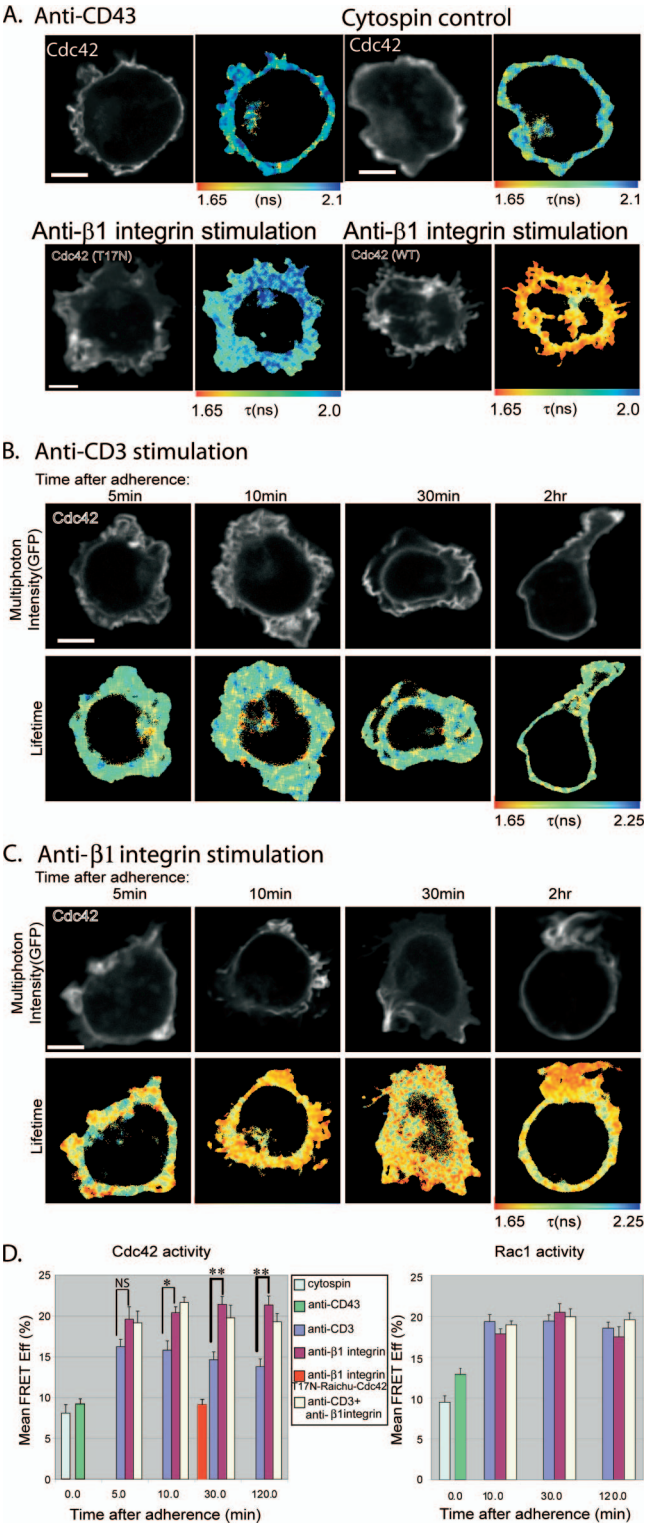

FIG. 1. Cdc42 is differentially activated via CD3 or β1 integrin, whereas Rac1 activity shows no significant difference between these stimuli. Shown are the multiphoton FLIM measurements of the intramolecular FRET between GFP and mRFP1 in the mRFP-Raichu-Cdc42-GFP1 biosensor in Jurkat T cells that were spread on antibody-coated coverslips for up to 2 h before fixation. (A) Upper left, nonstimulating anti-CD43 MAb (30 min only); upper right, nonadhered control cell that has been fixed in suspension and subsequently cytospun onto a coverslip; lower left, T17N-mutated Raichu-Cdc42 on anti-β1 integrin MAb (12G10; 30 min); lower right, Raichu-Cdc42 on anti-β1 integrin MAb (12G10; 30 min). (B) Time course upon stimulation by anti-CD3 (UCHT1)-activating antibody. (C) Time course upon stimulation by anti-β1 integrin-activating antibody (MAb 12G10). An increase in probe activity and, therefore, FRET between GFP and mRFP1 results in the shortening of the fluorescence lifetime (τ) of GFP. The cell images of fluorescence intensity were thresholded to remove the autofluorescent background and areas of the cell that do not have sufficient photon counts for fitting with the exponential models described (50). The *x-z* section of a Raichu-Cdc42-expressing cell that has been costained with a membrane dye (1,1′-dioctadecyl tetramethyl indodicarbcyanine 4-chlorobenzenesulfonate salt [DiD]) shows that the Raichu probe is localized predominantly in the membrane (see Fig. S1 in the supplemental material). (D) Bar charts showing the cumulative data of four experiments ($n = 15$ cells) and five experiments ($n = 17$ cells) for Cdc42 and Rac1 Raichu biosensors, respectively (NS, not significant; ∗, $P < 0.05$; ∗∗, $P < 0.005$; all by *t* test). The mean FRET efficiency in each cell (with the total number of pixels normalized to 1) is calculated by the equation FRET Eff $= 1 - \tau_{da}/\tau_d$, where τ_{da} is the lifetime of GFP molecules interacting with acceptor and τ_d is GFP lifetime in the absence of acceptor (GFP-Cdc42 control; not shown). The averages (per cell) of the mean FRET efficiency values ± standard errors of the means of cells expressing Raichu-Cdc42 or Raichu-Rac1 at each time point are presented. Scale bars = 5 μm.

adherence on anti-β1 integrin, from 9.1% ± 0.6% to 21.5% ± 1.4% (Fig. 1 A, D). This time point was chosen on the basis of the maximum difference between the anti-β1- and anti-CD3-induced Cdc42 activities observed in Fig. 1D.

Taken together, these results indicate that a higher level of Cdc42 activity can be achieved by β1 integrin activation than by CD3 activation in T cells. In contrast, Rac1 activity is increased equally by activation through either β1 integrin or CD3.

Receptor-stimulated Cdc42 activity is dependent on ERM activity. Members of the ERM family of proteins play an important regulatory role during IS formation (18, 58) and T-cell activation by aiding the formation of the DPC (15). In our current T-cell model, there appears to be a mechanism that activates Cdc42 differently in accordance with the nature of the receptor (CD3 or integrin). This is supported by two recent findings. Previously, we demonstrated that the localized activation of Cdc42 in breast carcinoma cells is due to the involvement of the activated/phosphorylated form of ezrin in recruiting the Rho/Cdc42-specific GEF Dbl to the membrane as well as the subsequent activation of Cdc42, not Rac1 (53). Similarly, in lymphocytes, both the C-terminal threonine-phosphorylated form of ERM and the phosphomimetic (T567D) ezrin mutant have been found to coprecipitate with Dbl (31). These data lead us to postulate that the receptor specificity is achieved through an ERM-dependent mechanism. We therefore investigated the role of ezrin in Cdc42 and Rac1 activation.

ERM proteins have two domains separated by an extended alpha-helical domain, namely N-ERMAD (NH2-terminal ERM association domain) and C-ERMAD (COOH-terminal ERM association domain). The activation of ezrin requires the phosphorylation of threonine residue T567 in the C-ERMAD (22), an effect that can be mimicked by a T567D point mutation. The N-terminal domain of ezrin has a dominant inhibitory effect on ERM activity, which is enhanced by a single-amino-acid substitution (E244K) (53). WT and mutant ezrin

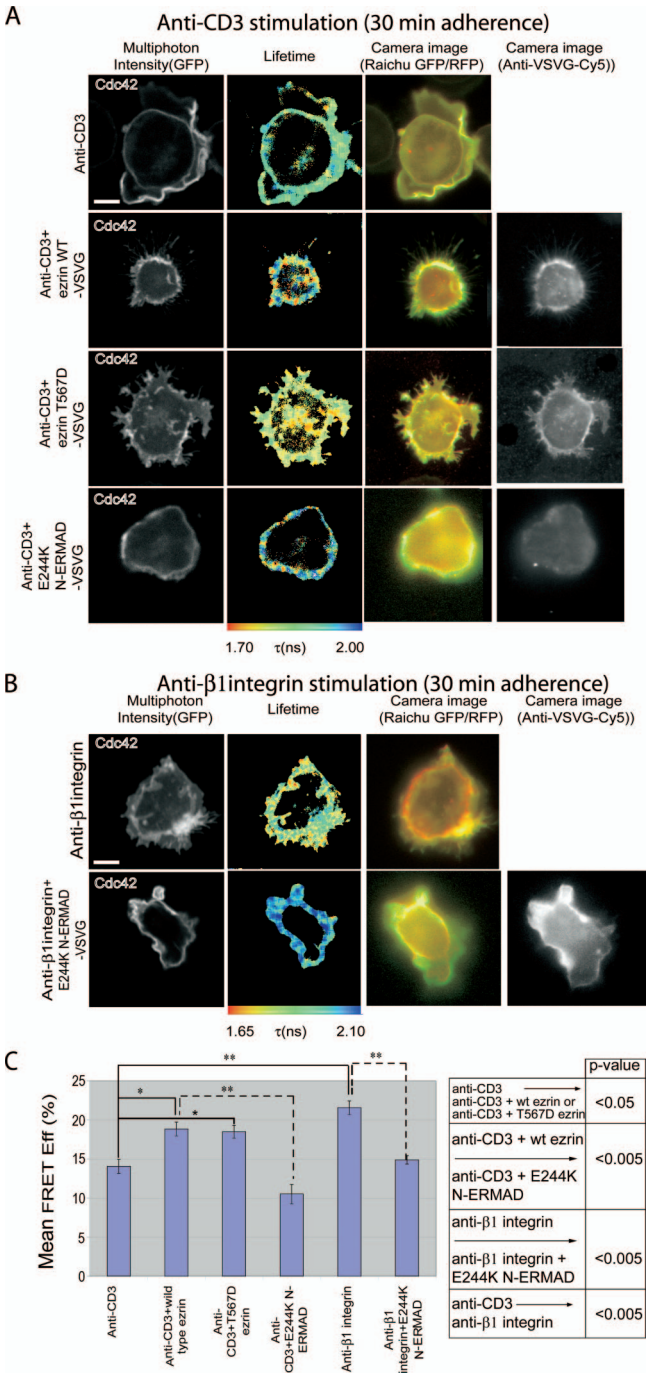

FIG. 2. Receptor-stimulated Cdc42 activity is dependent on ERM activity. Jurkat cells were transfected with Raichu-Cdc42, either alone or with the indicated ezrin (VSV-G-tagged) construct, and allowed to adhere to anti-CD3 (UCHT1) (A) or anti-β1 integrin (12G10) (B) antibody-coated coverslips for 30 min at 37°C before fixation. Exogenous ezrin expression was detected by staining (following cell fixation and permeabilization) with a Cy5-conjugated anti-VSV-G IgG. (C) Bar charts represent the cumulative data of three experiments ($n = 10$ cells error bars ± standard errors of the means). We compared each treatment group to the controls and other groups by one-way analysis of variance (ANOVA). If the ANOVA indicated a significant difference between groups, a pairwise multiple comparison of all means and post hoc testing using Tukey's method were employed to determine significant differences between groups and controls. The table summarizes the P values derived from one-way ANOVA with post hoc statistical analysis (*, $P < 0.05$; **, $P < 0.005$). Scale bars = 5 μm.

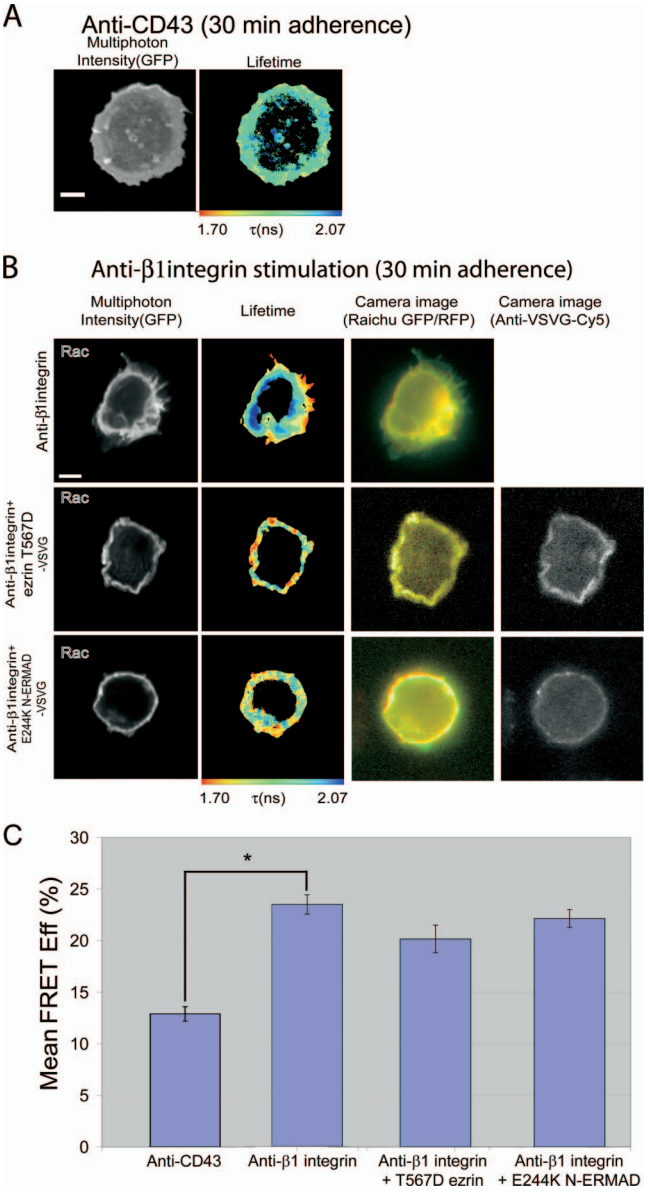

FIG. 3. Receptor-stimulated Rac1 activity is not affected by ezrin activity. Jurkat cells were transfected with Raichu-Rac, either alone or with the indicated ezrin (VSV-G-tagged) construct, and then allowed to adhere to anti-CD43 (A) or anti-β1 integrin (12G10) (B) antibody-coated coverslips for 30 min at 37°C before fixation. For panel B, ezrin expression was detected by staining (following cell fixation and permeabilization) with a Cy5-conjugated anti-VSV-G IgG. (C) Bar charts represent the cumulative data of two independent experiments ($n = 9$ cells; *, $P < 0.05$). Scale bars = 5 μm.

were VSV-G tagged and overexpressed in Jurkat cells with the Raichu biosensors. The expression of both the WT and T567D forms significantly increased the Cdc42 activity in anti-CD3-stimulated cells ($P < 0.05$) to levels close to that achieved by anti-β1 integrin activation (Fig. 2A, C). The dominant inhibition of endogenous ERM activity by E244K N-ERMAD significantly reduced both CD3- and β1 integrin-induced Cdc42 activation ($P < 0.005$) (Fig. 2A to C). However, β1 integrin-induced Rac1 activation was insensitive to the expression of

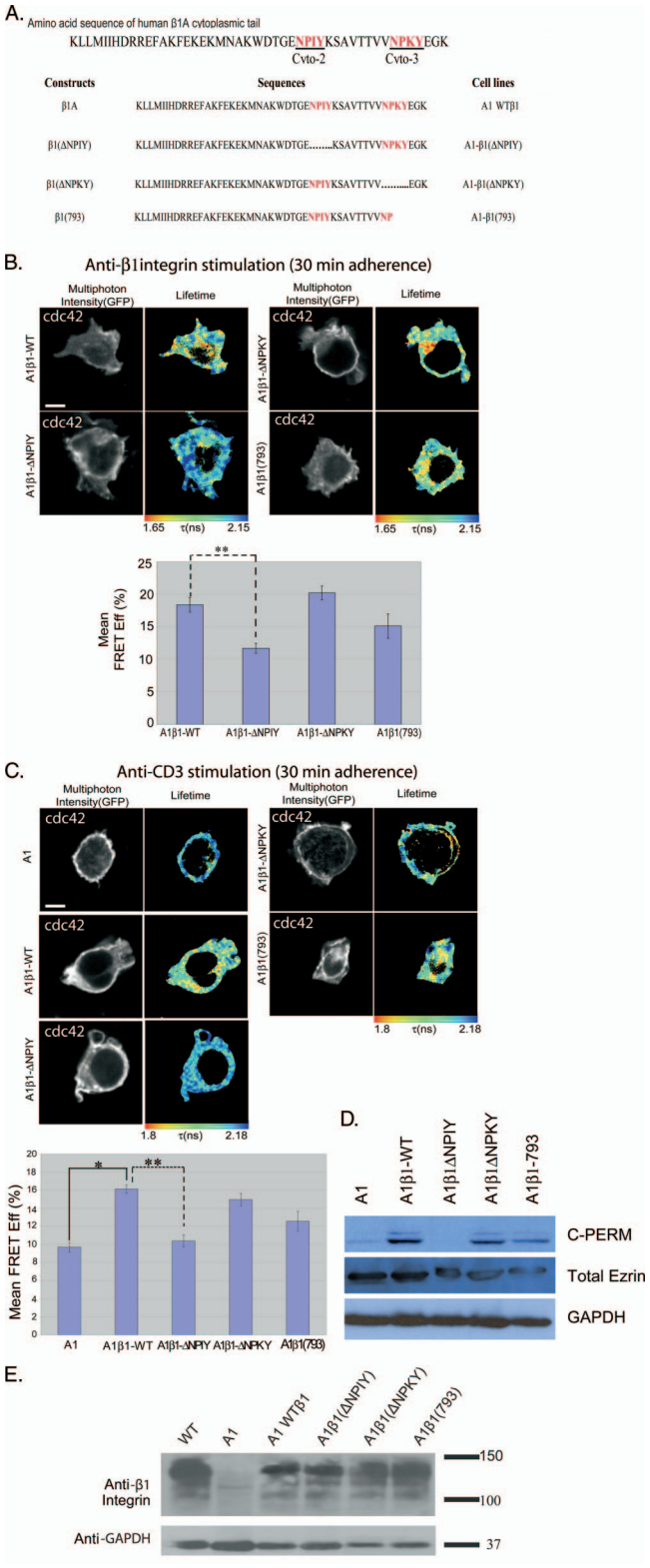

FIG. 4. NPIY motif of β1 integrin is important for Cdc42 activation. The β1 integrin-deficient A1 cells and the various A1-derived lines that have been reconstituted with the WT and mutated β1 integrin constructs (sequences summarized in panel A, where …… depicts the deleted regions) were adhered on anti-β1 integrin (12G10) (B) or anti-CD3 (UCHT1) (C) antibody-coated coverslips for 30 min at 37°C. This time point was chosen on the basis of the maximum difference between anti-β1- and anti-CD3-induced Cdc42 activities observed from the data in Fig. 1D. Bar charts represent the cumulative FLIM/FRET data of three experiments ($n = 7$ cells) (*, $P < 0.05$; **, $P < 0.005$). Scale bar = 5 μm. (D) Western blot analysis of whole-cell lysates from A1 cells and the various β1 integrin-reconstituted A1-derived lines. Blots were probed with anti-C-PERM (ERM phosphorylated at the conserved threonine residue in the COOH terminus) rabbit IgG (Cell Signaling) or anti-total ezrin (an in-house MAb, 2H3) antibody as described before (53). (E) Western blot analysis of whole-cell lysates from A1 cells and the various β1 integrin-reconstituted A1-derived lines. Blots were probed with an anti-total β1 integrin antibody (MAb 8E3; a kind gift of Martin Humphries, University of Manchester). Results shown are representative of two independent experiments.

E244K N-ERMAD and remained high (Fig. 3). This is consistent with our hypothesis that ezrin is involved in the preferential activation of Cdc42, but not Rac1, via the membrane recruitment of a Cdc42-GEF and Rho-GEF, Dbl (53).

The NPIY motif of β1 integrin is important for Cdc42 activation. It has been demonstrated that integrins act upstream of Cdc42 during the directed migration of astrocytes (17). The molecular basis for β1 integrin-induced Cdc42 activation is not well characterized, and this pathway has not, to our knowledge, been demonstrated in T cells. We investigated the β1 integrin dependence of Cdc42 and Rac1 activities using the A1 mutant Jurkat T-cell line. This was isolated initially due to its inability to bind fibronectin after phorbol ester dibutyrate treatment and subsequently was found to be β1 integrin deficient (56). We also investigated A1 cells reconstituted with the WT (A1β1-WT) and a number of cytoplasmic mutants of β1 integrin (Fig. 4A). The relative expression levels for the transfection of various β1 integrin constructs in the β1-null A1 cells are provided in Fig. 4E. Consistently with the published findings, A1 cells were unable to adhere to anti-β1 integrin antibody-coated coverslips. We found a significant ($P < 0.005$) reduction in FRET efficiency with the Cdc42 Raichu probe in A1β1-ΔNPIY cells compared to that of A1β1-WT cells adhered to anti-β1 integrin antibody-coated coverslips (Fig. 4B). This demonstrates that the membrane-proximal NPXΦ motif, containing the talin-binding site in both β1 (13) and β2 (36) integrins, is important for integrin-mediated Cdc42 activation. Similarly, we observed an inability of anti-CD3 stimulation to trigger Cdc42 activity in β1-deficient A1 cells. This was restored in A1β1-WT, A1β1-ΔNPKY, and A1β1-793 cells. Cdc42 activity was not restored in A1β1-ΔNPIY cells ($P < 0.005$), indicating that the same membrane-proximal NPXΦ motif is important for anti-CD3-stimulated activation (Fig. 4C).

We have shown that ERM activity is necessary for receptor-stimulated Cdc42 activity (Fig. 2). To determine the involvement of specific β1 integrin cytoplasmic domains in Rho GTPase activation, we examined the levels of the phosphorylation/activity of endogenous ERM proteins in the different A1 lines. Both cell lines with impaired Cdc42 responses to β1 integrin stimulation, A1 and A1β1-ΔNPIY cells (Fig. 4B), also exhibited a reduction in basal C-ERMAD phosphorylation compared to that of A1β1-WT, A1β1-ΔNPKY, and A1β1-793 cells (Fig. 4D).

Signaling cross-talk exists between LFA-1 and β1 integrin in T lymphocytes (52). We considered whether LFA-1 integrin

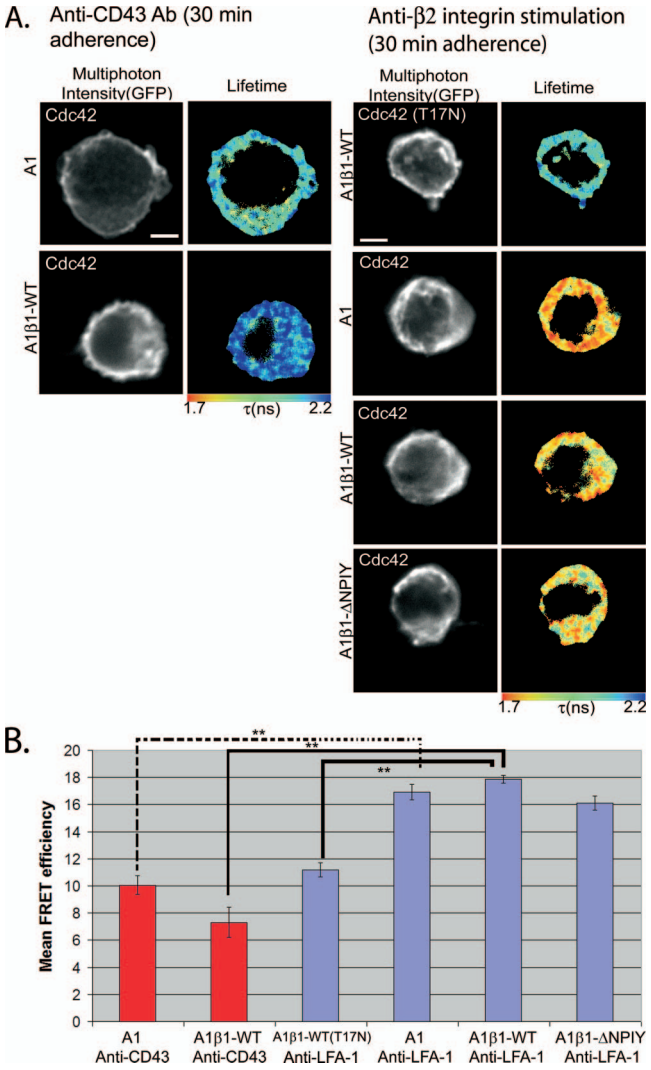

FIG. 5. Input to trigger Cdc42 activity is derived from both β1 and β2 integrins in T cells. (A) The β1-integrin-deficient A1 cells and A1-derived lines that have been reconstituted with the WT or mutant β1 integrin constructs were transfected with Raichu-Cdc42 (or the T17N mutant) and adhered on anti-CD43 (left) or anti-LFA-1 (right) antibody-coated coverslips for 30 min at 37°C. (B) Bar charts represent the cumulative FLIM/FRET data of three experiments ($n = 7$ cells). FRET/FLIM analysis as described for Fig. 1. **, $P < 0.005$ by t test. Scale bars = 5 μm.

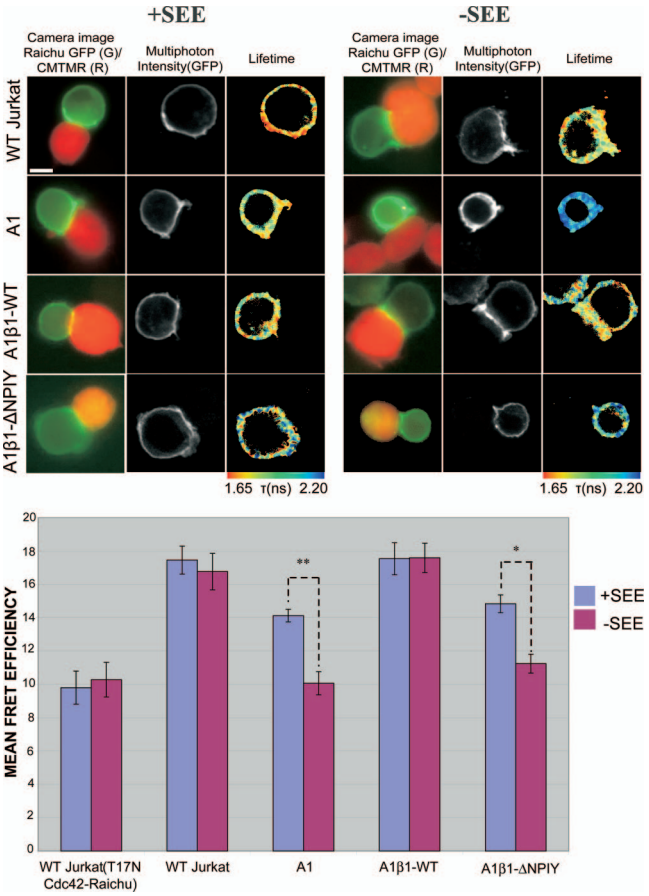

FIG. 6. SEE-induced Cdc42 activation at the IS with Raji APC. Jurkat T cells (WT or A1-derived lines) expressing the Raichu-Cdc42 plasmid were added to Raji B cells either preloaded with SEE superantigen (+SEE) or unloaded as a control (−SEE). WT Jurkat cells transfected with the T17N mutant form of Raichu-Cdc42 provide the baseline control. Target cells were labeled for 15 min at 37°C with 20 μM CMTMR (orange cell tracking dye; Molecular Probes). The mRFP1 emission was not visible at the set exposure time for the red channel, which was kept at a minimum because of the brightness of the CMTMR labeling. Bar charts represent the cumulative data of four experiments ($n = 15$ cells) for Raichu-Cdc42 (*, $P < 0.05$; **, $P < 0.005$; both by t test). Scale bar = 5 μm.

stimulation can compensate for the lack of β1 integrin by eliciting Cdc42 activation in β1-deficient A1 cells. We observed a baseline level of FRET when A1 or A1β1-WT cells were adhered to anti-CD43-coated coverslips as an unstimulated but adhered control (Fig. 5A). When these cells were spread on a coverslip surface precoated with an anti-CD11a (LFA-1) antibody, a significant ($P < 0.005$) increase in FRET efficiency was observed in both the A1 and A1β1-WT (and A1β1-ΔNPIY) cells (Fig. 5). This increase in FRET efficiency by anti-LFA-1 stimulation indicates that the input to trigger Cdc42 activity is derived from both β1 and β2 integrins in T cells. The implication of these findings for IS formation is discussed below.

SEE-induced Cdc42 activation at the IS with Raji APC. We next examined the significance of our findings in the IS, where multiple receptors may contribute (synergistically or independently) to Rho GTPase activation. We used a T-cell activation model in which contacts between T cells and APC are made in the presence or absence of the SEE superantigen. In the absence of SEE, both A1 and A1β1-ΔNPIY cells formed only loose contacts with the APC, and the mean FRET efficiency was similar to that observed in WT Jurkat cells transfected with the T17N mutant Raichu-Cdc42 (Fig. 6). The presentation of the superantigen significantly increased and partially restored the Cdc42 activities in both A1 and A1β1-ΔNPIY cells (Fig. 6). As this activity may be due to the stimulatory effect of CD11a engagement (Fig. 5), we examined the localization of both β1 integrin and LFA-1 in the conjugates. Both were shown to be significantly enriched (but not exclusively localized) at the IS formed by WT Jurkat cells with APC, particularly in the presence of SEE, in agreement with a previous report (39) (Fig. 7B). Furthermore, the ability of β1-deficient Jurkat (A1) cells to form conjugates with APC was

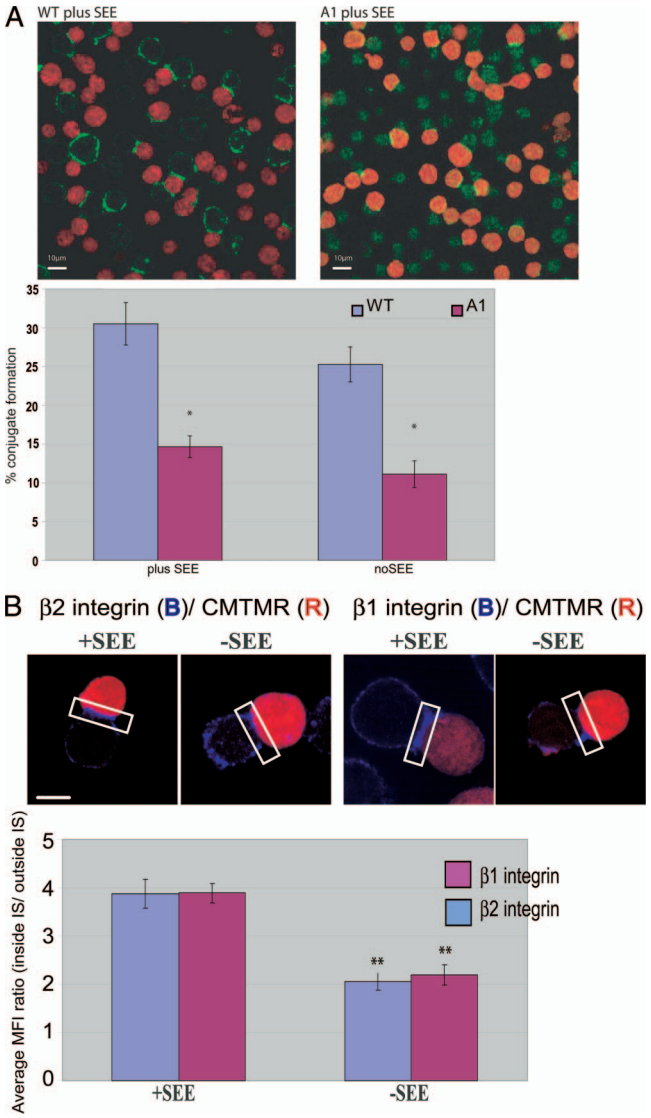

FIG. 7. Conjugation and integrin accumulation at the IS with Raji APC. (A) Raji cells were labeled with CMTMR orange dye and incubated in the presence or absence of the superantigen SEE. WT or β1 integrin-deficient Jurkat (A1) cells were incubated at a 1:1 ratio with CMTMR-stained Raji (red) for 30 min at 37°C. The conjugates were fixed in solution and stained with anti-LFA-1 integrin (green). The graph shows the percentage of WT and A1 conjugates; the percent conjugates is the number of conjugates in a field/total number cells in field for each cell line. The data were collected from three independent experiments ($n = 10$ fields). Each bar presents the percent conjugates ± standard errors of the means. Asterisks indicate any statistically significant difference between the WT and A1 cells in the presence or absence of superantigen (*, $P < 0.005$). Scale bars = 10 μm. (B) Raji cells were labeled with CMTMR and incubated in the presence or absence of the superantigen SEE. WT Jurkat T cells were incubated at a 1:1 ratio with CMTMR-stained Raji (red) for 30 min at 37°C. The conjugates were fixed in solution and stained for β1 integrin or LFA-1 and then analyzed by confocal microscopy. The graph shows the manually masked mean fluorescence intensity (MFI) ratio at the membrane only (inside IS/outside IS). The data were collected from three independent experiments ($n = 12$ cells). Each bar presents the mean fluorescence intensities ± standard errors of the means. (**, $P < 0.005$ by t test for the difference between −SEE and +SEE for both integrin subtypes). Scale bar = 5 μm.

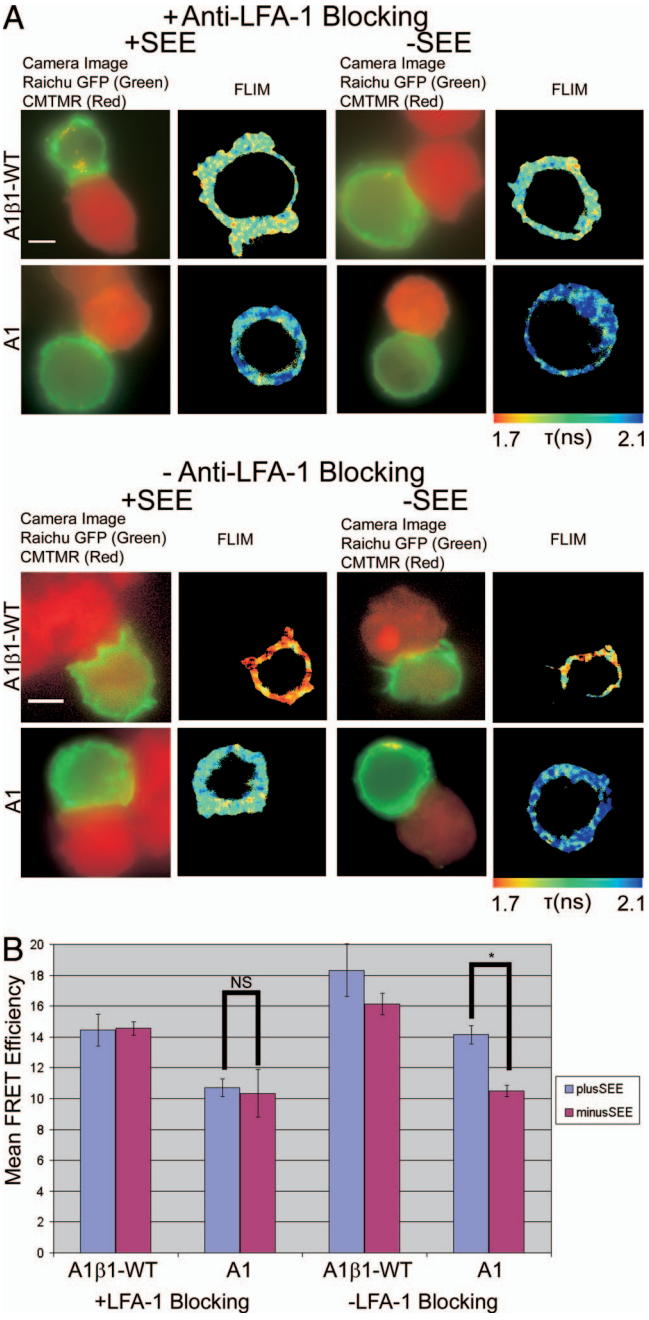

FIG. 8. LFA-1 blocking returns Cdc42 activity in β1 integrin-deficient cells to a baseline level at the IS with SEE-loaded Raji APC. (A) A1β1-WT and A1 cells either were preblocked for 45 min at 37°C with 10 μg/ml blocking anti-LFA-1 MAb (MAb 38; Cancer Research United Kingdom Antibody service) or were incubated without blocking MAb. The T cells then were allowed to form conjugates with SEE-loaded or unloaded CMTMR-stained Raji APC as described for Fig. 7. (B) Bar chart showing cumulative FLIM/FRET data for Raichu-Cdc42 in A1β1-WT and A1 cells forming conjugates with Raji APC with and without LFA-1 blocking antibody treatment ($n = 17$ cells). Scale bars = 5 μm. NS, not significant; *, $P < 0.05$; both by t test.

reduced by ~50% (Fig. 7A). In A1 cells that did manage to form conjugates with APC, the assembly of an IS was able to proceed (as indicated by LFA-1 recruitment to the contact site). Finally, the blocking of LFA-1 in A1 cell (but not

A1β1-WT cell) conjugates formed in the presence of SEE reduced Cdc42 activity compared to that observed without SEE treatment (Fig. 8). This indicates that LFA-1 partially compensates for the absence of β1 integrins by contributing to Cdc42 activation at the IS.

DISCUSSION

In this report we have documented that, in both CD3- and β1 integrin-stimulated cells, Cdc42 activity is dependent on the cyto-2 (NPIY) motif of the β1 integrin cytoplasmic domain. Also, both receptors require the phosphorylated/activated ERM to sustain Cdc42 (but not Rac1) activity. This is supported by experiments using a dominant inhibitory ezrin construct and the finding that ERM C-terminal threonine phosphorylation is impaired in cells that are deficient in β1 integrin or express the Δcyto-2 (NPIY) form of the receptor. This implies that both IS-associated receptors lie on the same (serial) molecular pathway and transduce signals through the ERM-dependent machinery that is responsible for the remodeling of the cytoskeleton and the stabilization of the synapse. Previous reports by us and others suggested that the recruitment of Dbl (a Rho/Cdc42-specific GEF) by activated ezrin is involved in Cdc42 activation (31, 53). Note that there are cell type-specific differences in the wiring of the regulatory elements (GEFs and GAPs) linking the ERM proteins to the various Rho GTPases. This is clearly illustrated in the demonstration of the signaling of activated ezrin to Rac1, but not to Cdc42 or RhoA, in Madin-Darby canine kidney cells (54).

Our future research will focus on the identification of the GEF(s) responsible for the integrin- and ERM-dependent activation of Cdc42. There are >80 GEFs and >70 GAPs in the genome for regulating the 22 mammalian Rho GTPases (55). There is, therefore, redundancy and potential for cross-compensation among the different GEFs. Other GEFs probably are implicated in the regulation of Cdc42 activity in our system in addition to Dbl. For instance, PIXα has been shown to be required for chemoattractant-mediated Cdc42 (not Rac1) and PAK1 activation in mouse neutrophils (35). Similarly, previous publications have inferred a role for Cdc42 in PAK activation downstream of a stable trimolecular complex of PAK1, PIX, and the paxillin kinase linker p95PKL. Furthermore, the authors suggested that this Cdc42- and PAK-activating complex is recruited via integrins (29, 51).

Cdc42 activity is impaired in β1 integrin-deficient T cells that form conjugates with APC. However, the use of both β1 integrin-deficient A1 and A1 reconstituted with the cyto-2 (NPIY) deletion mutant of β1 integrin demonstrates that other molecules, such as LFA-1, can activate Cdc42 and thereby induce the cytoskeletal rearrangements that are necessary for synapse formation (59). The data here indicate that LFA-1 can partially compensate for the absence of β1 integrins via Cdc42 activation at the IS. These results are consistent with other reports on the various lipid raft-dependent (34) and cytoskeleton-dependent (33) cross-compensatory activities between β1 (α4β1 and α4β1) and β2 integrins.

There are technical difficulties associated with imaging T cells that are triggered by APC within the context of an antigen-dependent synapse or by an APC-mimicking stimulatory substrate. There is a significant time delay between the onset of cell-cell contact and paraformaldehyde fixation. There is also a delay between the initial few minutes of cell adhesion onto substrate and the stage at which the Raichu activities can be observed in cells that are in stable contact with the antibody-coated glass surface. According to the simulation in Fig. S2C in the supplemental material, regardless of the initial GEF concentration, the theoretical time to achieve a maximum degree of Cdc42 activation in response to a specific stimulus is ~12 s. This is incompatible with our experiments, making it impossible to resolve the rate of the initial rise of the FRET population F_2. It is interesting that the time to equilibrium (10 to 15 s) is similar to that obtained from another modeling study of the activation dynamics of the heterotrimeric G proteins (37). Despite using multiphoton excitation, which vastly improved the z resolution (14, 30), the FRET population (GTP-Cdc42) (Fig. 6) was not localized exclusively to the synapse site, even in the WT Jurkat cells. It is likely that different subpopulations of the GTPases are involved in an ongoing surveillance function through, for example, the actin-rich forward-probing membrane structures (15) that are around, but separate from, the site of synapse with the APC. The alternative possibility is that the GTP-Cdc42 species diffuses rapidly from the synapse site.

We observed a small decrease in the FRET population (see Fig. S2 in the supplemental material) over time for the anti-CD3-stimulated T cells. This may represent the dissociation of the GEF from the site of activation. Since anti-CD3 stimulation has been shown to induce ERM dephosphorylation in T cells (18), this may contribute to the time-dependent dissociation of GEF. A previous model consisting of Jurkat cells adhering to a stimulatory substrate (a glass surface precoated with stimulatory antibodies) has shown a direct correlation between the polarization of the microtubule-organizing center toward the APC-mimicking stimulatory substrate and a redistribution of the TcR to the bottom of the cell attached to the substrate (3). Since Cdc42 is linked through its downstream effectors to microtubule-organizing center polarization (6), the difference in the rate of decrease of Cdc42-GTP (k_{off}) according to the nature of the receptor engaged may exert feedback on the recruitment of the antigen receptor to the cell-substratum interface. This contributes to a more-rapid signal termination process following CD3 stimulation compared to that for β1 integrin.

β1 integrin engagement has been shown to activate Cdc42 in astrocytes (17), but the mechanisms involved have not been demonstrated. β1 integrins have been shown to cofractionate with ezrin upon PKC activation (42). The observed correlation between cyto-2 deletion and the ERM C-terminal threonine phosphorylation state provides a novel mechanism that links β1 integrin to Cdc42 activation. But how does the deletion of the cyto-2 (NPIY) motif affect β1 integrin-induced Rho GTPase activation? The binding of talin to integrin disrupts an intracellular salt bridge between the α and β subunits, leading to increased integrin affinity for ligand. Integrin binding to talin has been shown to correlate with its ability to induce FAK phosphorylation (11). Both the phosphatidylinositol 4′-phosphate-5′-kinase (PIPK) and the NPIY motif of β1 integrin bind to the same surface of the talin FERM (band 4.1, ERM) domain (9). Therefore, the increased production of phosphatidylinositol 4,5-biphosphate (PIP2) by the PIPK recruited by the integrin-talin complex may be responsible for the confor-

mational activation of ERM proteins and consequently the binding of PIP2 to the FERM domain of ERM (20). β2 integrins have been shown to recruit RhoA in Cos-7 cells during phagocytosis (61). Residues 758 to 760 (TTT), situated between the two NPXΦ motifs in β2 integrin (similar $VT^{792}T^{793}$ residues are conserved in β1 integrin), are required for this function. β1 integrins also can modulate the activity of Rho GTPases such as RhoA via p190RhoGAP (4). Future work focusing on the effect of β1 integrin signaling on GAP proteins that are specific to Cdc42 will enable us to further refine the mechanistic model and thereby provide new insights into the regulation of the Rho GTPase cycling network.

ACKNOWLEDGMENTS

K. Makrogianneli is supported by a joint research studentship from MRC/King's College London. L. Carlin and D. Matthews are supported by a United Kingdom EPSRC grant (EP/C546105/1). Enyinnaya Ofo is a recipient of both a Wellcome Trust Clinical Training Fellowship and the Dimbleby Cancer Care Award. M. Keppler, S. Ameer-Beg, and T. Ng are supported by an endowment fund from Dimbleby Cancer Care to King's College London. A. Coolen is the recipient of a Springboard Research Fellowship from EPSRC. The multiphoton FLIM system was built with support from both the Medical Research Council Co-Operative Group grant (G0100152 ID 56891) and an United Kingdom Research Councils Basic Technology Research Programme grant (GR/R87901/01).

We thank Anne Ridley and Hannah Gould (Randall Division, KCl), Peter Parker and John Maher (Division of Cancer Studies, KCl), Giovanna Lombardi (MRC Centre in Transplantation, KCl), and Federica Marelli-Berg (Imperial College London) for reviewing the manuscript and providing helpful comments and suggestions. We also thank Nancy Hogg (Cancer Research United Kingdom, London Research Institute) for her advice on the use of anti-LFA-1 blocking antibodies.

REFERENCES

1. **Algrain, M., O. Turunen, A. Vaheri, D. Louvard, and M. Arpin.** 1993. Ezrin contains cytoskeleton and membrane binding domains accounting for its proposed role as a membrane-cytoskeletal linker. J. Cell Biol. **120:**129–139.
2. **Anilkumar, N., M. Parsons, R. Monk, T. Ng, and J. C. Adams.** 2003. Interaction of fascin and protein kinase C a: a novel regulatory intersection in cell adhesion and motility. EMBO J. **22:**5390–5402.
3. **Arkhipov, S. N., and I. V. Maly.** 2006. Quantitative analysis of the role of receptor recycling in T cell polarization. Biophys. J. **91:**4306–4316.
4. **Arthur, W. T., L. A. Petch, and K. Burridge.** 2000. Integrin engagement suppresses RhoA activity via a c-Src-dependent mechanism. Curr. Biol. **10:**719–722.
5. **Avizienyte, E., M. Keppler, E. Sandilands, V. G. Brunton, S. J. Winder, T. Ng, and M. C. Frame.** 2007. An active Src kinase-beta-actin association is linked to actin dynamics at the periphery of colon cancer cells. Exp. Cell Res. **313:**3175–3188.
6. **Banerjee, P. P., R. Pandey, R. Zheng, M. M. Suhoski, L. Monaco-Shawver, and J. S. Orange.** 2007. Cdc42-interacting protein-4 functionally links actin and microtubule networks at the cytolytic NK cell immunological synapse. J. Exp. Med. **204:**2305–2320.
7. **Barber, P., S. M. Ameer-Beg, J. Gilbey, R. J. Edens, I. Ezike, and B. Vojnovic.** 2005. Global and pixel kinetic data analysis for FRET detection by multi-photon time-domain FLIM. Proc. SPIE **5700:**171–181.
8. **Barber, P. R., S. M. Ameer-Beg, J. Gilbey, L. M. Carlin, M. Keppler, T. C. Ng, and B. Vojnovic.** 2008. Multiphoton time-domain fluorescence lifetime imaging microscopy: practical application to protein-protein interactions using global analysis. J. R. Soc. Interface. **6:**S93–S105.
9. **Barsukov, I. L., A. Prescot, N. Bate, B. Patel, D. N. Floyd, N. Bhanji, C. R. Bagshaw, K. Letinic, G. Di Paolo, P. De Camilli, G. C. Roberts, and D. R. Critchley.** 2003. Phosphatidylinositol phosphate kinase type 1gamma and beta1-integrin cytoplasmic domain bind to the same region in the talin FERM domain. J. Biol. Chem. **278:**31202–31209.
10. **Cannon, J. L., and J. K. Burkhardt.** 2004. Differential roles for Wiskott-Aldrich syndrome protein in immune synapse formation and IL-2 production. J. Immunol. **173:**1658–1662.
11. **Chen, H. C., P. A. Appeddu, J. T. Parsons, J. D. Hildebrand, M. D. Schaller, and J. L. Guan.** 1995. Interaction of focal adhesion kinase with cytoskeletal protein talin. J. Biol. Chem. **270:**16995–16999.
12. **Dadke, S., S. Cotteret, S. C. Yip, Z. M. Jaffer, F. Haj, A. Ivanov, F. Rauscher III, K. Shuai, T. Ng, B. G. Neel, and J. Chernoff.** 2007. Regulation of protein tyrosine phosphatase 1B by sumoylation. Nat. Cell Biol. **9:**80–85.
13. **Dedhar, S., and G. E. Hannigan.** 1996. Integrin cytoplasmic interactions and bidirectional transmembrane signalling. Curr. Opin. Cell Biol. **8:**657–669.
14. **Dustin, M. L.** 2007. Cell adhesion molecules and actin cytoskeleton at immune synapses and kinapses. Curr. Opin. Cell Biol. **19:**529–533.
15. **Dustin, M. L.** 2004. Stop and go traffic to tune T cell responses. Immunity **21:**305–314.
16. **Dustin, M. L., and J. A. Cooper.** 2000. The immunological synapse and the actin cytoskeleton: molecular hardware for T cell signaling. Nat. Immunol. **1:**23–29.
17. **Etienne-Manneville, S., and A. Hall.** 2001. Integrin-mediated activation of Cdc42 controls cell polarity in migrating astrocytes through PKCzeta. Cell **106:**489–498.
18. **Faure, S., L. I. Salazar-Fontana, M. Semichon, V. L. Tybulewicz, G. Bismuth, A. Trautmann, R. N. Germain, and J. Delon.** 2004. ERM proteins regulate cytoskeleton relaxation promoting T cell-APC conjugation. Nat. Immunol. **5:**272–279.
19. **Feig, L. A., and G. M. Cooper.** 1988. Inhibition of NIH 3T3 cell proliferation by a mutant ras protein with preferential affinity for GDP. Mol. Cell. Biol. **8:**3235–3243.
20. **Fievet, B. T., A. Gautreau, C. Roy, L. Del Maestro, P. Mangeat, D. Louvard, and M. Arpin.** 2004. Phosphoinositide binding and phosphorylation act sequentially in the activation mechanism of ezrin. J. Cell Biol. **164:**653–659.
21. **Ganesan, S., S. M. Ameer-beg, T. T. C. Ng, B. Vojnovic, and F. S. Wouters.** 2006. A dark yellow fluorescent protein (YFP)-based resonance energy-accepting chromoprotein (REACh) for Forster resonance energy transfer with GFP. Proc. Natl. Acad. Sci. USA **103:**4089–4094.
22. **Gautreau, A., D. Louvard, and M. Arpin.** 2002. ERM proteins and NF2 tumor suppressor: the Yin and Yang of cortical actin organization and cell growth signaling. Curr. Opin. Cell Biol. **14:**104–109.
23. **Gautreau, A., D. Louvard, and M. Arpin.** 2000. Morphogenic effects of ezrin require a phosphorylation-induced transition from oligomers to monomers at the plasma membrane. J. Cell Biol. **150:**193–203.
24. **Hoffman, G. R., N. Nassar, and R. A. Cerione.** 2000. Structure of the Rho family GTP-binding protein Cdc42 in complex with the multifunctional regulator RhoGDI. Cell **100:**345–356.
25. **Hogg, N., M. Laschinger, K. Giles, and A. McDowall.** 2003. T-cell integrins: more than just sticking points. J. Cell Sci. **116:**4695–4705.
26. **Ilani, T., C. Khanna, M. Zhou, T. D. Veenstra, and A. Bretscher.** 2007. Immune synapse formation requires ZAP-70 recruitment by ezrin and CD43 removal by moesin. J. Cell Biol. **179:**733–746.
27. **Itoh, R. E., K. Kurokawa, Y. Ohba, H. Yoshizaki, N. Mochizuki, and M. Matsuda.** 2002. Activation of rac and cdc42 video imaged by fluorescent resonance energy transfer-based single-molecule probes in the membrane of living cells. Mol. Cell. Biol. **22:**6582–6591.
28. **Khurana, D., and P. J. Leibson.** 2003. Regulation of lymphocyte-mediated killing by GTP-binding proteins. J. Leukoc. Biol. **73:**333–338.
29. **Ku, G. M., D. Yablonski, E. Manser, L. Lim, and A. Weiss.** 2001. A PAK1-PIX-PKL complex is activated by the T-cell receptor independent of Nck, Slp-76 and LAT. EMBO J. **20:**457–465.
30. **Kurokawa, K., R. E. Itoh, H. Yoshizaki, Y. O. Nakamura, and M. Matsuda.** 2004. Coactivation of rac1 and cdc42 at lamellipodia and membrane ruffles induced by epidermal growth factor. Mol. Biol. Cell **15:**1003–1010.
31. **Lee, J. H., T. Katakai, T. Hara, H. Gonda, M. Sugai, and A. Shimizu.** 2004. Roles of p-ERM and Rho-ROCK signaling in lymphocyte polarity and uropod formation. J. Cell Biol. **167:**327–337.
32. **Legg, J. W., C. A. Lewis, M. Parsons, T. Ng, and C. M. Isacke.** 2002. A novel PKC-regulated mechanism controls CD44 ezrin association and directional cell motility. Nat. Cell Biol. **27:**399–407.
33. **Leitinger, B., and N. Hogg.** 2000. Effects of I domain deletion on the function of the beta2 integrin lymphocyte function-associated antigen-1. Mol. Biol. Cell **11:**677–690.
34. **Leitinger, B., and N. Hogg.** 2002. The involvement of lipid rafts in the regulation of integrin function. J. Cell Sci. **115:**963–972.
35. **Li, Z., M. Hannigan, Z. Mo, B. Liu, W. Lu, Y. Wu, A. V. Smrcka, G. Wu, L. Li, M. Liu, C. K. Huang, and D. Wu.** 2003. Directional sensing requires G beta gamma-mediated PAK1 and PIX alpha-dependent activation of Cdc42. Cell **114:**215–227.
36. **Lim, J., A. Wiedemann, G. Tzircotis, S. J. Monkley, D. R. Critchley, and E. Caron.** 2007. An essential role for talin during alpha(M)beta(2)-mediated phagocytosis. Mol. Biol. Cell **18:**976–985.
37. **Mahama, P. A., and J. J. Linderman.** 1994. A Monte Carlo study of the dynamics of G-protein activation. Biophys. J. **67:**1345–1357.
38. **Miletic, A. V., M. Swat, K. Fujikawa, and W. Swat.** 2003. Cytoskeletal remodeling in lymphocyte activation. Curr. Opin. Immunol. **15:**261–268.
39. **Mittelbrunn, M., A. Molina, M. M. Escribese, M. Yanez-Mo, E. Escudero, A. Ursa, R. Tejedor, F. Mampaso, and F. Sanchez-Madrid.** 2004. VLA-4 integrin concentrates at the peripheral supramolecular activation complex of the immune synapse and drives T helper 1 responses. Proc. Natl. Acad. Sci. USA **101:**11058–11063.

40. **Morton, P., T. Ng, S. A. Roberts, B. Vojnovic, and S. M. Ameer-Beg.** 2003. Time-resolved multiphoton imaging of the interaction between the PKC and the NFkB cell signalling pathway. Progr. Biomed. Optics Imaging **4:**216–222.
41. **Nakamura, T., K. Aoki, and M. Matsuda.** 2005. Monitoring spatio-temporal regulation of Ras and Rho GTPase with GFP-based FRET probes. Methods **37:**146–153.
42. **Ng, T., M. Parsons, W. E. Hughes, J. Monypenny, D. Zicha, A. Gautreau, M. Arpin, S. Gschmeissner, P. J. Verveer, P. I. Bastiaens, and P. J. Parker.** 2001. Ezrin is a downstream effector of trafficking PKC-integrin complexes involved in the control of cell motility. EMBO J. **20:**2723–2741.
43. **Ng, T., D. Shima, A. Squire, P. I. H. Bastiaens, S. Gschmeissner, M. J. Humphries, and P. J. Parker.** 1999. PKCa regulates b1 integrin-dependent motility, through association and control of integrin traffic. EMBO J. **18:** 3909–3923.
44. **Ng, T., A. Squire, G. Hansra, F. Bornancin, C. Prevostel, A. Hanby, W. Harris, D. Barnes, S. Schmidt, H. Mellor, P. I. Bastiaens, and P. J. Parker.** 1999. Imaging protein kinase Cα activation in cells. Science **283:**2085–2089.
45. **Ng, T. T., I. E. Collins, S. B. Kanner, M. J. Humphries, N. Amft, R. G. Wickremasinghe, D. D'Cruz, K. E. Nye, and W. J. Morrow.** 1999. Integrin signalling defects in T-lymphocytes in systemic lupus erythematosus. Lupus **8:**39–51.
46. **Ng, T. T., S. B. Kanner, M. J. Humphries, R. G. Wickremasinghe, K. E. Nye, J. Anderson, S. H. Khoo, and W. J. Morrow.** 1997. The integrin-triggered rescue of T lymphocyte apoptosis is blocked in HIV-1-infected individuals. J. Immunol. **158:**2984–2999.
47. **Parsons, M., M. D. Keppler, A. Kline, A. Messent, M. J. Humphries, R. Gilchrist, I. R. Hart, C. Quittau-Prevostel, W. E. Hughes, P. J. Parker, and T. Ng.** 2002. Site-directed perturbation of PKC-integrin interaction blocks carcinoma cell chemotaxis. Mol. Cell. Biol. **22:**5897–5911.
48. **Parsons, M., J. Monypenny, S. M. Ameer-Beg, T. H. Millard, L. M. Machesky, M. Peter, M. D. Keppler, G. Schiavo, R. Watson, J. Chernoff, D. Zicha, B. Vojnovic, and T. Ng.** 2005. Spatially distinct binding of Cdc42 to PAK1 and N-WASP in breast carcinoma cells. Mol. Cell. Biol. **25:**1680–1695.
49. **Perez, O. D., S. Kinoshita, Y. Hitoshi, D. G. Payan, T. Kitamura, G. P. Nolan, and J. B. Lorens.** 2002. Activation of the PKB/AKT pathway by ICAM-2. Immunity **16:**51–65.
50. **Peter, M., S. M. Ameer-Beg, M. K. Hughes, M. D. Keppler, S. Prag, M. Marsh, B. Vojnovic, and T. Ng.** 2005. Multiphoton-FLIM quantification of the EGFP-mRFP1 FRET pair for localization of membrane receptor-kinase interactions. Biophys. J. **88:**1224–1237.
51. **Phee, H., R. T. Abraham, and A. Weiss.** 2005. Dynamic recruitment of PAK1 to the immunological synapse is mediated by PIX independently of SLP-76 and Vav1. Nat. Immunol. **6:**608–617.
52. **Porter, J. C., and N. Hogg.** 1997. Integrin cross talk: activation of lymphocyte function-associated antigen-1 on human T cells alters alpha4beta1- and alpha5beta1-mediated function. J. Cell Biol. **138:**1437–1447.
53. **Prag, S., M. Parsons, M. D. Keppler, S. M. Ameer-Beg, P. Barber, J. Hunt, A. J. Beavil, R. Calvert, M. Arpin, B. Vojnovic, and T. Ng.** 2007. Activated ezrin promotes cell migration through recruitment of the GEF Dbl to lipid rafts and preferential downstream activation of Cdc42. Mol. Biol. Cell **18:** 2935–2948.
54. **Pujuguet, P., L. Del Maestro, A. Gautreau, D. Louvard, and M. Arpin.** 2003. Ezrin regulates E-cadherin-dependent adherens junction assembly through Rac1 activation. Mol. Biol. Cell **14:**2181–2191.
55. **Ridley, A. J.** 2006. Rho GTPases and actin dynamics in membrane protrusions and vesicle trafficking. Trends Cell Biol. **16:**522–529.
56. **Romzek, N. C., E. S. Harris, C. L. Dell, J. Skronek, E. Hasse, P. J. Reynolds, S. W. Hunt III, and Y. Shimizu.** 1998. Use of a beta1 integrin-deficient human T cell to identify beta1 integrin cytoplasmic domain sequences critical for integrin function. Mol. Biol. Cell **9:**2715–2727.
57. **Rosenthal-Allieri, M. A., M. Ticchioni, J. P. Breittmayer, Y. Shimizu, and A. Bernard.** 2005. Influence of beta 1 integrin intracytoplasmic domains in the regulation of VLA-4-mediated adhesion of human T cells to VCAM-1 under flow conditions. J. Immunol. **175:**1214–1223.
58. **Roumier, A., J. C. Olivo-Marin, M. Arpin, F. Michel, M. Martin, P. Mangeat, O. Acuto, A. Dautry-Varsat, and A. Alcover.** 2001. The membrane-microfilament linker ezrin is involved in the formation of the immunological synapse and in T cell activation. Immunity **15:**715–728.
59. **Salazar-Fontana, L. I., V. Barr, L. E. Samelson, and B. E. Bierer.** 2003. CD28 engagement promotes actin polymerization through the activation of the small Rho GTPase Cdc42 in human T cells. J. Immunol. **171:**2225–2232.
60. **Spitaler, M., E. Emslie, C. D. Wood, and D. Cantrell.** 2006. Diacylglycerol and protein kinase D localization during T lymphocyte activation. Immunity **24:**535–546.
61. **Wiedemann, A., J. C. Patel, J. Lim, A. Tsun, Y. van Kooyk, and E. Caron.** 2006. Two distinct cytoplasmic regions of the beta2 integrin chain regulate RhoA function during phagocytosis. J. Cell Biol. **172:**1069–1079.
62. **Woolf, E., I. Grigorova, A. Sagiv, V. Grabovsky, S. W. Feigelson, Z. Shulman, T. Hartmann, M. Sixt, J. G. Cyster, and R. Alon.** 2007. Lymph node chemokines promote sustained T lymphocyte motility without triggering stable integrin adhesiveness in the absence of shear forces. Nat. Immunol. **8:**1076–1085.
63. **Wouters, F. S., and P. I. Bastiaens.** 1999. Fluorescence lifetime imaging of receptor tyrosine kinase activity in cells. Curr. Biol. **9:**1127–1130.
64. **Wouters, F. S., P. J. Verveer, and P. I. Bastiaens.** 2001. Imaging biochemistry inside cells. Trends Cell Biol. **11:**203–211.
65. **Zaidel-Bar, R., S. Itzkovitz, A. Ma'ayan, R. Iyengar, and B. Geiger.** 2007. Functional atlas of the integrin adhesome. Nat. Cell Biol. **9:**858–867.